Turk J Phys
36 (2012) , 207 – 213.

doi:10.3906/fiz-1106-8

TE surface waves in dielectric slab sandwiched between LHM slabs

Ass'ad I. ASS'AD[1] and Hassan S. ASHOUR[2]
[1] *Department of Physics at Al-Aqsa University, Gaza Strip-PALESTINIAN AUTHORITY*
e-mail: assad_assad11@yahoo.com
[2] *Department of Physics at Al-Azhar University-Gaza, Gaza Strip-PALESTINIAN AUTHORITY*
e-mail: hashour@alazhar.edu.ps

Received: 16.06.2011

Abstract

In this work, the dispersion relation for TE surface waves has been derived for a slab waveguide constructed from a dielectric material slab sandwiched between two thick layers of left-handed material (LHM). The dispersion relation and the power flow were numerically solved for a given set of parameters: the structural factor, dielectric slab thickness, and the operating frequency on the effective refractive index and power flow. We found that the wave effective refractive index decreases with thickness increase as well as increase in frequency. We found that the effective refractive index increases slightly with increase of structural factor. Also, the power flow increases with thickness and increases with operating frequency.

Key Words: TE surface waves, dispersion relation, left-handed metamaterial, power flow

1. Introduction

Great interest is focused on the propagation of electromagnetic waves in artificial materials, particularly of materials with negative index of refraction; materials which are designed to exhibit both negative permeability and permittivity over predetermined range of frequencies. In those materials, one needs to consider the wave vector, the electric field, and the magnetic field form a left-handed system. Thus, they are called left-handed materials (LHM). A group of researchers at the University of San Diego have been able to synthesize an artificial dielectric medium from such materials (metamaterials). They were able to demonstrate that those materials exhibit both negative dielectric permittivity and magnetic permeability simultaneously over a certain range of frequencies [1]. That work realized the prediction of Veselago in his pioneer paper [2] describing electromagnetic propagation in an isotropic medium with negative dielectric permittivity $\varepsilon(\omega) < 0$ and negative permeability $\mu(\omega) < 0$ could exhibit unusual properties. Understanding such LHM materials requires detailed understanding of the electric field vector E, the magnetic field vector H, and the wave vector k, together forming a left-hand

orthogonal set [3, 4]. The recent demonstrations on the existence of the LHM opened wide unique possibilities in the design of novel devices based on electromagnetic wave propagation in such materials, but in a non-conventional way.

Since most communication devices (e.g., waveguides and microstrips) include dielectric materials, we were motivated to investigate a three layered structure of dielectric material slab between two thick layers of left-handed material (LHM). Metamaterials are used in fabricating Transmission lines [5, 6], microstrip resonators [7], couplers [8], resonators [9], and antennas [10].

These applications motive us to investigate the propagation of TE waves in a three-layer structure composed of a single dielectric material layer sandwiched between two layers of LHM metamaterial. The goal is to develop towards potential applications in fabricating antenna, microstrips, and couplers.

Remainder of this paper is organized as follows. Section 2 we derive the dispersion relation of the surface waves in LHM-Dielectric-LHM structure and the power flow. In Section 3 we discuss the numerical results. Section 4 is solely devoted to the conclusion.

2. Theory

2.1. The dispersion relation

We briefly outline the derivation of the dispersion relation for TE surface waves in the structure. The dispersion relation for TE wave propagation in the x-axis with propagation wave constant β is represented in the form $e^{ik_0(\beta x-ct)}$, where$\beta = k/k_0$, k is the effective wave index; and k_0 is the free space wave number, which equals ω/c , where c is the velocity of light, and ω is the applied angular frequency. Figure 1 shows the geometry and coordinates of the structure under investigation. The structure is a dielectric material $(0 < y < t)$ bounded between two thick layers of left-handed material. The electromagnetic field components are

$$E = [0, E_y, 0] \exp\left(ik_0\left(\beta x - ct\right)\right) , \tag{1}$$

$$H = [H_x, 0, H_z] \exp\left(ik_0\left(\beta x - ct\right)\right) . \tag{2}$$

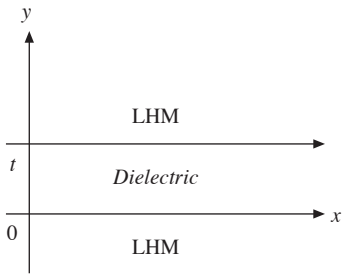

Figure 1. The geometry of the problem.

2.1.1. In linear dielectric region $(0 < y < t)$

Substitution of equations (1) and (2) into Maxwell's equation yields the following linear differential equation to satisfy in the linear dielectric slab:

$$\frac{\partial^2 E_y}{\partial z^2} - k_0^2(\beta^2 - \epsilon\mu)E_y = 0, \tag{3}$$

The solution of equation (3) is given by

$$E_{y2} = A\sinh(k_2 z) + B\cosh(k_2 z), \tag{4}$$

where $k_2 = k_0\sqrt{\beta^2 - \epsilon\mu}$. The magnetic field components in the linear dielectric are

$$H_{x2} = -(i/\omega\mu_0)\, k_2 \left[A\cosh(k_2 z) + B\sinh(k_2 z)\right], \tag{5}$$

$$H_{z2} = -(k/\omega\mu_0)\left[A\sinh(k_2 z) + B\cosh(k_2 z)\right]. \tag{6}$$

2.1.2. In LHM regions ($y > t$ and $y < 0$)

Substitution of equations (1) and (2) into Maxwell's equation yields the following differential equation to satisfy in the LHM slab:

$$\frac{\partial^2 E_y}{\partial z^2} - k_0^2\left(\beta^2 - \varepsilon_{eff}\mu_{eff}\right) E_y = 0, \tag{7}$$

where, ε_{eff} and μ_{eff} are the effective lossless dielectric permittivity and permeability respectively, and they given as, [11–15]

$$\varepsilon_{eff} = 1 - \frac{\omega_p^2}{\omega^2} \tag{8}$$

and

$$\mu_{eff} = 1 - \frac{F\omega^2}{\omega^2 - \omega_0^2}. \tag{9}$$

Here, ω_p is the plasma angular frequency of the wires, ω is the operating angular frequency, F is the structural factor which depends on the characteristics of the embedded split rings resonators SRR in host material, and ω_0 is the resonant frequency of the split ring resonators.

The solution to equation (7) is

$$E_{y3} = Ce^{k_3 z}, \tag{10}$$

where

$$k_1^2 = k_0^2\left(\beta^2 - \varepsilon_{eff}\mu_{eff}\right)$$

and β is the effective refractive index.

The magnetic field components in the cover at $y > t$ are

$$H_{x3} = -\left(\frac{i}{\omega\mu_0\mu_{eff}}\right) Ck_3 e^{k_3 z}, \tag{11}$$

$$H_{z3} = -\left(\frac{k}{\omega\mu_0\mu_{eff}}\right) Ae^{k_3 z}. \tag{12}$$

The dispersion relation can be found by matching the field components at the interface $y = 0$ and $y = t$, that is

$$\tanh(k_2 t) = \frac{Rk_2 - k_1}{Rk_1 - k_2}, \tag{13}$$

where $R = \frac{k_1}{k_2\mu_{eff}}$.

2.2. Power flow

The power flux of the TE surface waves along the direction of propagation can be found by integrating the Poynting vector

$$P = \frac{1}{2}\int (E \times H^*)\, dz = \frac{1}{2}\int E_y H_z dz = P_{1LHM} + P_D + P_{2LHM}\,, \tag{14}$$

$$P_D = \frac{1}{2}(k/\omega\mu o)B^2[P_{1D} + P_{2D} + P_{3D}], \tag{15}$$

where,

$$B = e^{-k_1 t}[R\sinh(k_2 t) + \cosh(k_2 t)]^{-1}$$

$$P_{1D} = R^2(\cosh(k_2 t)\sinh(k_2 t) - k_2 t)/(2k_2)$$

$$P_{2D} = (\cosh(k_2 t)\sinh(k_2 t) + k_2 t)/(2k_2)$$

$$P_{3D} = (R\sinh^2(k_2 t))/k_2$$

$$P_{LHM} = \frac{1}{4}\left(\frac{k}{k_2\omega\mu_0\mu_{eff}}\right)B^2. \tag{16}$$

3. Results and discussion

The dispersion relation (13) is numerically solved to find the effective wave index β as a function of the angular frequency ω for different dielectric constants, and for different values of dielectric film thicknesses (t = 20, 40, 60, 80 and 100 μm). The power flux for the structure under investigation has been investigated as a function of film thicknesses. The parameters of the LHM are adjusted so that the permittivity and permeability are negative in the frequency range 10.3∼10.5 GHz. The parameters used in the numerical calculations are: ω_p = 25 GHz, ε = 88, and ω_0 = 10.21 GHz.

In Figure 2, we plot the effective refractive indexβ as a function of the operating frequency for different dielectric slab thickness. It is noticed that the effective refractive index decreases smoothly with frequency. Thus, the overall effect of structure behaves like a left-handed material (LHM), since the slope of the dispersion relation represents the group velocity [16]. A negative gradient means that the group velocity is negative, which ensures that the structure behaves like a LHM. These properties are due to the fact that the Poynting vector in the LHM is anti-parallel to the wave number, which is characterized by a negative dielectric constant [17, 18].

The effective refractive index of the structure as a function of the dielectric constant of the dielectric slab at different film thickness and at angular frequency is shown in Figure 3. We notice that the effective refractive indexβ of the structure smoothly decreases with increase in the dielectric constant. We noticed that the effective refractive index decreases smoothly with increase in the dielectric constant. The effective refractive index is found to decrease with increase in dielectric slab thickness for all dielectric constant values. It is well known that the dielectric constant changes due to many external parameters, i.e. pressure, temperature, as well as operating frequency [19–21]. Thus, the change in the effective refractive index value, due to the change in the slab thickness, may be useful in designing pressure or temperature sensors.

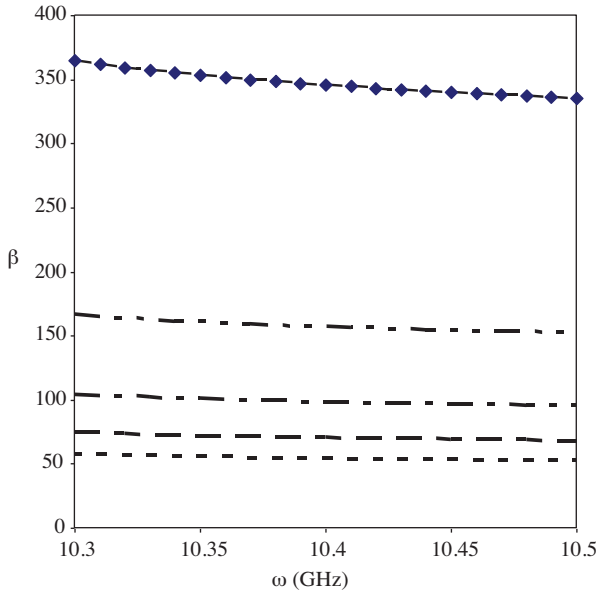

Figure 2. The effective refractive index versus the angular frequency for different dielectric slab thicknesses. The upper diamond-dash curve is for 20 μm thickness and the lowest dotted curve is for 100 μm.

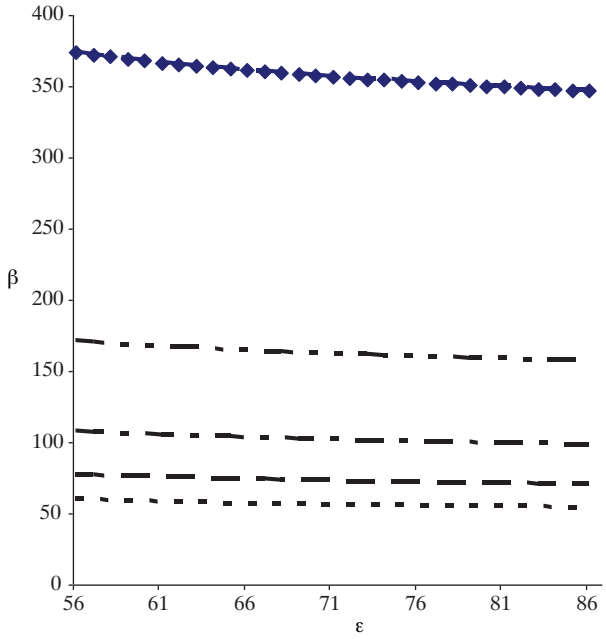

Figure 3. The effective refractive index versus the dielectric constant of the dielectric slab, at $\omega = 10.4$ GHz for different dielectric slab thicknesses. The upper diamond-dash curve is for 20 μm thickness and the lowest dotted curve is for 100 μm.

In Figure 4 we plotted the effective refractive index β versus the structural factor F of the split ring resonator (SRR) at for different dielectric slab thickness. We notice that the effective refractive index smoothly increases with structural factor. This monotonic smooth increase gives us flexibility in designing the SRR.

Figure 5 shows the normalized power flow (P/P_0), where $P_0 = 1/(2\varepsilon_0\omega)$, as a function of the operating frequency with dielectric constant $\epsilon = 88$. At low frequencies, the power flow decreases with increase in frequency. The power flow is sensitive to dielectric medium slab thickness, increasing with slab thickness.

In Figure 6, we plotted the power as a function of the dielectric constant of the dielectric slab, for different slab thicknesses. We choose the operating frequency so that power flow exhibits decreases for dielectric constants and for all dielectric slab thicknesses. We notice that, from Figure 6, that the power flow has almost steep degradation at 100 μm thickness, and from Figure 2, we notice that the 100 μm thickness claims the lowest value of effective refractive index. This means that the highest response occurs at 100 μm thickness (low values of effective refractive index, β), but the highest power flow through the surface. Thus, this structure can be used to sense the change in some of the external parameters that affects the dielectric constant.

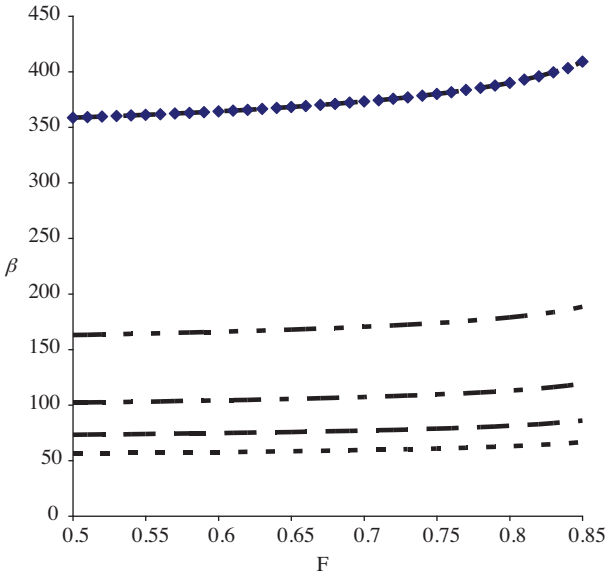

Figure 4. The effective refractive index versus the Split Ring Resonator (SRR) structural factor, F, with dielectric constant of the dielectric slab $\varepsilon = 60$, and operating frequency $\omega = 10.4$ GHz for different dielectric slab thicknesses. The upper diamond-dash curve is for 20 μm thickness and the lowest dotted curve is for 100 μm.

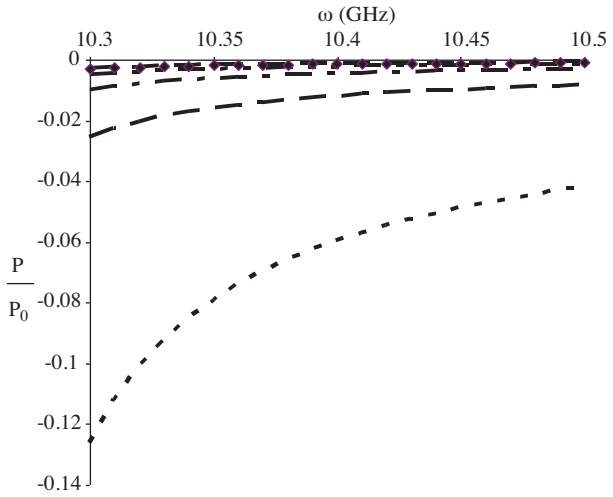

Figure 5. The normalized power flux versus the operating angular frequency with dielectric constant, $\varepsilon = 88$, for different dielectric slab thicknesses. The upper diamond-dash curve is for 20 μm thickness and the lowest dotted curve is for 100 μm.

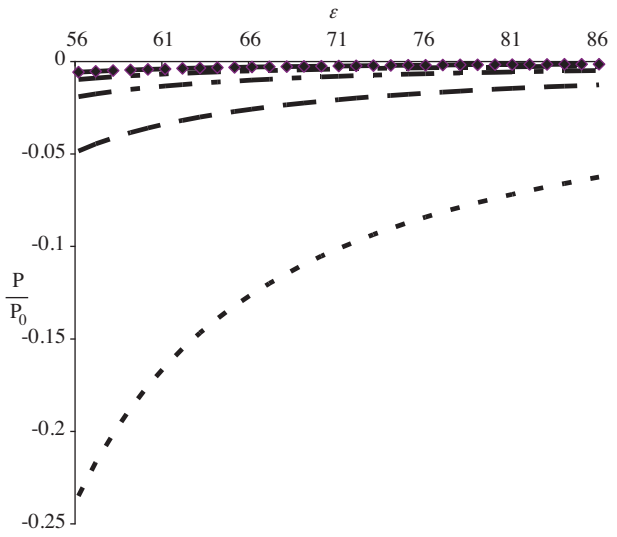

Figure 6. The normalized power flux versus the dielectric constant at operating angular frequency, $\omega = 10.4$ GHz, for different dielectric slab thicknesses. The upper diamond-dash curve is for 20 μm thickness and the lowest dotted curve is for 100 μm.

4. Conclusion

A design of a three layer waveguide has been introduced wherein a dielectric layer is sandwiched between two thick layers of left-handed materials. A dispersion relation for TE surface waves has been derived and numerically investigated. We found that the wave effective refractive index decreases with increase in frequency at certain range of frequencies. Also, we found that the effective refractive index increases slightly with increase in structural factor. The power flow increases with thickness and increases with operating frequency. The structure showed a sensing potential, which can be utilized in the construction of pressure or temperature sensors.

References

[1] R. Shelby, D. Smith, and S. Schultz, *Science Magazine,* **292**, (2001), 77.

[2] V. Veselago, *Sov. Phys. Usp.*, **10**, (1968), 509.

[3] R. Shelby, D. Smith, N. Nasser, and S. Schultz, *Appl. Phys. Lett.*, **78**, (2001), 489.

[4] J. Pendry, *Phys. Rev. Lett.*, **85**, (2000), 3966.

[5] C. Caloz, and T. Itoh*, Proc. IEEE-AP-S USNC/URSI National Radio Science Meeting*, **2**, (2002), 412**.**

[6] C. Caloz, and T. Itoh, IEEE Press and Wiley, (New York. 2005).

[7] C. Caloz, and T. Itoh, *IEEE Trans.*, **52**, (2004), 1159.

[8] C. Caloz, and T. Itoh, *IEEE Microwave Wireless Components Lett.,* **14**, (2004), 31.

[9] S. Otto, A. Rennings, C. Caloz, P. Waldow, I. Wolff, and T. Itoh, Proc. IEEE AP-S USNC/URSI National Radio Science Meeting, (Washington. 2005).

[10] A. Sanada, K. Murakami, I. Awai, H. Kubo, C. Caloz, and T. Itoh, Paper Presented at 34th European Microwave Conference, Amsterdam, (2004), 1341.

[11] Y. Chen, P. Fischer, and F. Wise, Quantum Electronics and Laser Science Conference, (2005).

[12] P. Markos, and C. Soukoulis, *Phys. Rev. E*, **65**, (2002), 8.

[13] I. Shadrivov, S. Morrison, and Y. Kivshar, *Optics Express*, **14**, (2006), 9344.

[14] J. Zhou, N. Eleftherios. E. Koschny, and M. Costas, C. Soukoulis, *Optics Letters*, **31**, (2006), 3620.

[15] J. Kong, *J. Electromagnetic Waves and Applications,* **15**, (2001), 1319.

[16] A. I. Ass'ad, H. S. Ashour, M. M. Shabat, *International Journal of Modern Physics*, **B 21**, (2007), 1951.

[17] M. Hamada, A. El-Astal, and M. Shabat, *International Journal of Microwave and Optical Technology*, **2**, (2007), 112.

[18] D. Mihalache, R. Nazmitdinove, and V. Fedyanin, *Sov. J. Nucl*, **20**, (1989), 86.

[19] P. Smith and D. Riehl, *Journal of Physics and Chemistry of Solids*, **35**, (1974), 1327.

[20] C. Andeen, D. Schuele, and J. Fontanella, *Phys. Rev.,* B**6**, (1972), 591.

[21] G. Samara and P. Peercy, *Phys. Rev.*, B**7**, (1973), 1131.